


History hydrodynamic torque transitions in oscillatory spinning of stick-slip Janus particles

Cite as: AIP Advances 9, 125113 (2019); <https://doi.org/10.1063/1.5131678>

Submitted: 15 October 2019 . Accepted: 20 November 2019 . Published Online: 16 December 2019

A. R. Premlata , and Hsien-Hung Wei



View Online



Export Citation



CrossMark

ARTICLES YOU MAY BE INTERESTED IN

[Self-propulsion of a sticky sphere partially covered with a surface slip velocity](#)

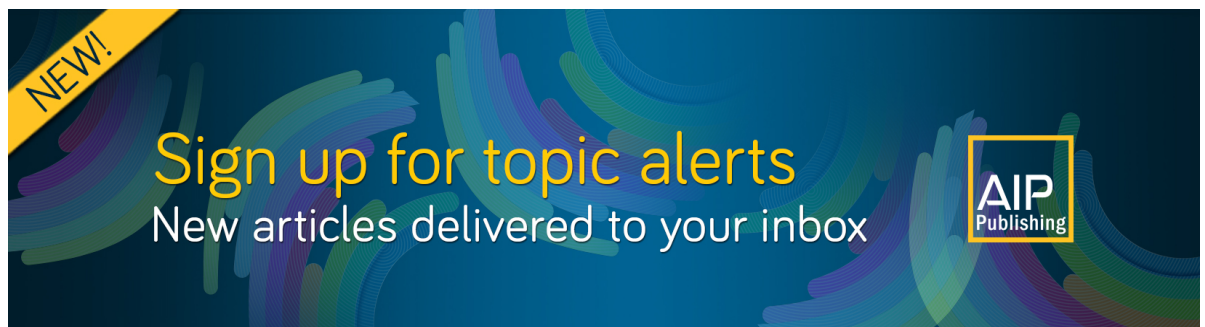
Physics of Fluids **31**, 112004 (2019); <https://doi.org/10.1063/1.5125567>

[Spontaneous autophoretic motion of isotropic particles](#)

Physics of Fluids **25**, 061701 (2013); <https://doi.org/10.1063/1.4810749>

[Inertial effects of self-propelled particles: From active Brownian to active Langevin motion](#)

The Journal of Chemical Physics **152**, 040901 (2020); <https://doi.org/10.1063/1.5134455>



NEW!

Sign up for topic alerts
New articles delivered to your inbox

AIP
Publishing

History hydrodynamic torque transitions in oscillatory spinning of stick-slip Janus particles

Cite as: AIP Advances 9, 125113 (2019); doi: 10.1063/1.5131678

Submitted: 15 October 2019 • Accepted: 20 November 2019 •

Published Online: 16 December 2019



View Online



Export Citation



CrossMark

A. R. Premrata  and Hsien-Hung Wei^{a)}

AFFILIATIONS

Department of Chemical Engineering, National Cheng Kung University, Tainan 701, Taiwan

^{a)} Author to whom correspondence should be addressed: hhwei@mail.ncku.edu.tw

ABSTRACT

We theoretically investigate the oscillatory spinning of an axisymmetric stick-slip Janus particle (SSJP) under the creeping flow condition. Solving the unsteady Stokes equation together with a matched asymptotic boundary layer theory, we find that such a particle can display unusual viscous torque responses in the high frequency regime depending on the Stokes boundary layer thickness δ , the slip length λ of the slip face, and the coverage of the stick face. Our analysis reveals that an SSJP will always experience a reduced Basset torque of $1/\delta$ decay due to the presence of the slip face, with amplitude smaller than the no-slip counterpart irrespective of the value of λ . If the coverage of the stick face is sufficiently small, the reduced Basset torque can turn into a constant torque plateau due to prevailing slip effects at larger values of δ , representing a new history torque transition prior to the slip-stick transition at $\delta \sim \lambda$. All these features are markedly different from those for no-slip and uniform slip particles, providing not only distinctive fingerprints for Janus particles but also a new means for manipulating these particles.

© 2019 Author(s). All article content, except where otherwise noted, is licensed under a Creative Commons Attribution (CC BY) license (<http://creativecommons.org/licenses/by/4.0/>). <https://doi.org/10.1063/1.5131678>

I. INTRODUCTION

A Janus particle is a compartmentalized colloid of two faces having distinct properties. It is commonly made of hydrophilic and hydrophobic caps, termed stick-slip Janus particle (SSJP). Because of its surface polarity, such a particle can work as an active cargo for expediting transport or be used to aid in colloidal assembly.¹ In addition, because the mobility of an SSJP can be further adjusted by the stick-slip partition, this may offer a tunable means to realize more precise hydrodynamic manipulations. While there are a few studies on the hydrodynamics of SSJP, they are mainly focused on the steady situation.^{2–8} The present work will be extended to the time-dependent scenario.

The present work is motivated by magnetically driven microrotors for generating rotational flows⁹ or by the use of rotating magnetic beads for biosensing applications.¹⁰ In the former, an SSJP could be a more efficient microrotor by having its slip portion faced down to the bottom wall to reduce drag. For the latter, a bead can be patched with a slip cap after absorbing hydrophobic proteins. This might affect its spinning behavior and hence the subsequent molecular transport on its surface. In either case, it is necessary to know

how much torque is needed to rotate an SSJP or how fast an SSJP can spin when it is subject to torsion. In the unsteady situation, since the applied torsion is not balanced by the viscous torque, the resulting rotational velocity may reveal more information about the particle. For rotary oscillations, since there exists a phase difference between the rotational velocity and the torque, the behavior of such phase difference for an SSJP is expected to vary with the stick-slip partition. This might provide a distinct fingerprint for an SSJP to differentiate from no-slip and uniform slip particles hydrodynamically.

As both no-slip and slip effects will join to influence the hydrodynamic responses of an SSJP, it is instructive to review basic features for no-slip and slip spheres under rotary oscillations. For a no-slip sphere, it is well known that it can experience a Basset history force¹¹ varying as a/δ due to a thin boundary layer of thickness $\delta = (2\nu/\omega)^{1/2}$, especially at the oscillation frequency ω much higher than the viscous damping frequency ν/a^2 , where a is the sphere radius and ν is the kinematic viscosity. More precisely, this a/δ Basset force arises from a much larger shear stress $\mu\Omega_0 a/\delta$ across the boundary layer with the peak angular velocity Ω_0 (with μ being the fluid viscosity). The resulting torque thus also varies as a/δ in the high ω regime.¹²

For a slip sphere, on the contrary, the boundary layer can become much thinner than the slip length λ at $\omega > \nu/\lambda^2$ to make slip effects much stronger. This leads to a constant shear stress $\mu\Omega_0 a/\lambda$ on the sphere surface.¹³ As a result, the torque also becomes constant and persists until the slip-stick transition (SST) point at $\delta \sim \lambda$ when $\omega \sim \nu/\lambda^2$ below which the usual Basset decay reappears.¹⁴ Such plateau and slip-stick transition are not noticed in the previous investigation on the unsteady rotation of a slippery sphere.¹⁵

As such, purely no-slip and slip particles have completely different characteristics in their torque responses. This raises a question, what if a particle is comprised of both no-slip and slip faces like an SSJP? In our recent study on an oscillatory translating SSJP,¹⁶ we found that the force response can be mixed with both no-slip and uniform slip contributions. While a similar torque response might be expected to occur to an oscillatory spinning SSJP, the two problems have quite distinct physics, reflected by the following aspects. First, for the translation problem the total viscous force on the particle is nonzero, whereas the spinning problem is force free. It follows that the flow field in the latter will decay at a much faster rate than that in the former. Second, for the translation problem, the added mass of $O((a/\delta)^2)$, which is purely of the potential flow origin, always exists in the force response.¹² However, there is no counterpart in the torque for the spinning problem since there is no net fluid entrainment by a force couple with a constant pressure everywhere.

Because of the above distinctions, the flow characteristics of the spinning problem are generally quite different from those of the translation problem. Such differences, in particular, manifest when there is a flow past a rotating sphere where a secondary flow emerges¹⁷ or in the nonvanishing Reynolds number situation where steady streaming often occurs.¹⁸ Prior to extending the uniform sphere situation to SSJP, it is necessary to analyze the leading order flow characteristics of SSJP under the Stokes flow condition. This is another reason why we would like to pursue this yet-explored spinning SSJP problem in this work.

II. PROBLEM FORMULATION

Motivated by the above, we consider the oscillatory spinning motion of a spherical SSJP of radius a at angular velocity $\Omega(t) = \Omega_0 e^{-i\omega t}$ in an incompressible viscous fluid of density ρ and viscosity μ , where Ω_0 is the peak angular velocity and ω is the oscillation frequency. As illustrated in Fig. 1, the particle is partially covered with a slip surface of polar angle θ_0 , with the remaining stick portion satisfying the no-slip boundary condition. Assume that the spinning is around the axis of the symmetry. Described by the spherical coordinates (r, θ, ϕ) with the origin at the center of the particle, the fluid velocity only occurs in the azimuthal ϕ direction. Having length, time, and velocity scaled by a , ω^{-1} , and $\Omega_0 a$, respectively, the azimuthal fluid velocity w' is governed by the unsteady Stokes equation in the dimensionless form,

$$\frac{\omega a^2}{\nu} \frac{\partial w'}{\partial t'} = \frac{1}{r^2} \frac{\partial}{\partial r} \left(r^2 \frac{\partial w'}{\partial r} \right) + \frac{1}{r^2} \sqrt{1-\eta^2} \frac{\partial^2}{\partial \eta^2} \left(\sqrt{1-\eta^2} w' \right), \quad (1)$$

with $\eta = \cos \theta$. Note that for this axisymmetric spinning, because the total viscous force on the particle is zero, the pressure is constant everywhere. Hence, there is no pressure term in (1).

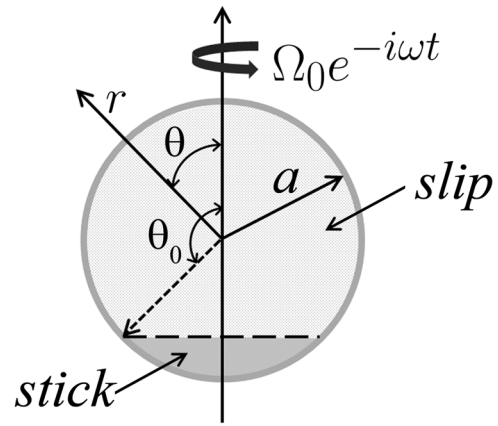


FIG. 1. Geometry of a spherical stick-slip Janus particle and coordinate system.

Transforming the problem into the frequency domain via $w' = w e^{-it'}$, Eq. (1) reads as

$$(E^2 - \alpha^2) \left(r \sqrt{1-\eta^2} w(r, \eta) \right) = 0, \quad (2)$$

where $E^2 = \partial_{rr} + r^{-2}(1-\eta^2)\partial_{\eta\eta}$ and $\alpha^2 = -i\omega a^2/\nu$ is the complex Womersley number with $\text{Re}\{\alpha\} > 0$. At the particle surface $r = 1$, the nonuniform slip boundary condition is prescribed,

$$w - \sqrt{1-\eta^2} = \beta(\eta) \tau_{r\phi}. \quad (3)$$

Here, $\beta(\eta)$ is the dimensionless slip parameter that can vary with η to account for the mixed stick-slip effects on the particle surface. $\beta = 0$ for the stick portion, whereas it turns into $\hat{\lambda} \equiv \lambda/a$ for the slip portion with the slip length λ . $\tau_{r\phi} = r\partial(w/r)/\partial r$ is the dimensionless shear stress scaled by $\Omega_0 \mu$.

The solution to (2) that satisfies (3) and $w \rightarrow 0$ as $r \rightarrow \infty$ takes the form

$$r \sqrt{1-\eta^2} w = \sum_{n=2}^{\infty} B_n R_n(r) G_n(\eta), \quad (4)$$

where $R_n(r) = r^{1/2} K_{n-1/2}(\alpha r)$ with $K_{n-1/2}$ being the modified Bessel functions of second kind and G_n are the Gegenbauer functions of degree $-1/2$. The coefficients B_n are determined by substituting (4) into (3) and by applying the orthogonality,

$$\int_{-1}^1 \frac{G_m(\eta) G_n(\eta)}{1-\eta^2} d\eta = \delta_{mn} C_n, \quad (5)$$

where δ_{nm} is the Kronecker delta and $C_n = 2/n(n-1)(2n-1)$. This yields the following infinite system of linear equations (via m) for B_n :

$$\sum_{n=2}^{\infty} B_n \{ R_n(1) C_n \delta_{mn} - L_{mn} (R_n'(1) - 2R_n(1)) \} = 2C_2 \delta_{m2}, \quad (6)$$

where

$$L_{mn} = \int_{-1}^1 \frac{G_m(\eta) G_n(\eta) \beta(\eta)}{1-\eta^2} d\eta.$$

For a given α , θ_0 , and $\hat{\lambda}$, (6) can be solved by truncation and matrix inversion. Convergent results can be obtained by retaining

100 terms. After finding B_n by solving (6), the shear stress on the particle can be determined as

$$\tau_{r\phi} = \sum_{n=2}^{\infty} B_n (R_n'(1) - 2R_n(1)) \frac{G_n(\eta)}{\sqrt{1-\eta^2}}. \quad (7)$$

The torque $T_z = T_z(\omega)e^{-i\omega t}$ acting on the particle can then be evaluated using

$$T_z = 2\pi a^3 \Omega_0 \mu \int_{-1}^1 \tau_{r\phi}|_{r=1} \sqrt{1-\eta^2} d\eta. \quad (8)$$

Using $\int_{-1}^1 G_n(\eta) d\eta = 2/3$ for $n = 2$ otherwise 0, we can determine the torque amplitude in (8) as

$$\frac{T_z(\omega)}{8\pi\mu\Omega_0 a^3} = \frac{1}{6} (R_2'(1) - 2R_2(1)) B_2. \quad (9)$$

Hence, only $n = 2$ mode in (4) contributes to the torque, which corresponds to an oscillating rotlet with $G_2(\eta) = (1 - \eta^2)/2$ and $R_2(r) = (\pi/2\alpha)^{1/2} (1 + (\alpha r)^{-1}) \exp(-\alpha r)$.

III. MIXED STICK AND SLIP TORQUE RESPONSES

First of all, it can be verified analytically that for constant β , (9) is reduced to the uniform slip result,¹⁴

$$\frac{T_z(\omega)}{-8\pi\mu\Omega_0 a^3} = \frac{\mathcal{T}}{1 + \sqrt{2}e^{-i\pi/4} \frac{1}{\delta} + 3\hat{\lambda}\mathcal{T}},$$

$$\mathcal{T} = 1 + \sqrt{2}e^{-i\pi/4} \frac{1}{\delta} + \frac{2}{3}e^{-i\pi/2} \frac{1}{\delta^2}. \quad (10)$$

Here, $\delta = (2\nu/\omega a^2)^{1/2}$ measures the extent of the boundary layer relative to the particle radius a . As revealed by (10), when the particle is no-slip with $\hat{\lambda} = 0$, the torque varies as $1/\delta$ as $\delta \rightarrow 0$ due to the Basset shearing with phase $\pi/4$ ahead of the particle rotational movement. In the case of uniform slip, however, the torque amplitude becomes a constant plateau of value $1/3\hat{\lambda}$ in the $\delta \rightarrow 0$ limit due to the constant shearing resulted from strong slip effects.¹⁴ Figure 2(a) plots the torque amplitude against $\hat{\delta}$ for a half cap SSJP ($\theta_0 = 90^\circ$). First of all, purely no-slip and uniform slip cases give torque amplitudes of $1/\delta$ and $1/3\hat{\lambda}$, respectively, as given by (10). As for a half cap SSJP, we find that all the curves with different values of $\hat{\lambda}$ tend to approach the same Basset-like $1/\delta$ decay as $\delta \rightarrow 0$, but in a reduced amplitude compared to the no-slip case due to drag reduction imparted by the slip face. Since such a Basset torque disappears when no-slip changes to uniform slip but reappears for an SSJP, it can be thought of as a *reentry* Basset torque to distinct from the usual no-slip Basset torque. In terms of the phase $\chi = \tan^{-1}[Im(T_z(\omega))/Re(T_z(\omega))]$, Fig. 2(b) shows that it basically varies from the no-slip result $\chi = -\pi/4$ to the uniform slip result $\chi = 0$ though changes can be nonmonotonic.

Figure 3(a) plots how the torque amplitude varies as gradually decreasing the stick portion by increasing θ_0 . When increasing θ_0 to 150° where the stick portion becomes small, we observe a *reentrant history torque transition* (RHTT) in which the torque first follows a Basset-like $1/\delta$ decay in the small δ regime and then turns into a slip plateau at larger values of δ prior to the SST point $\hat{\delta} \sim \hat{\lambda}$. How the phase χ varies with δ in this case appears even more nonmonotonic, as shown in Fig. 3(b).

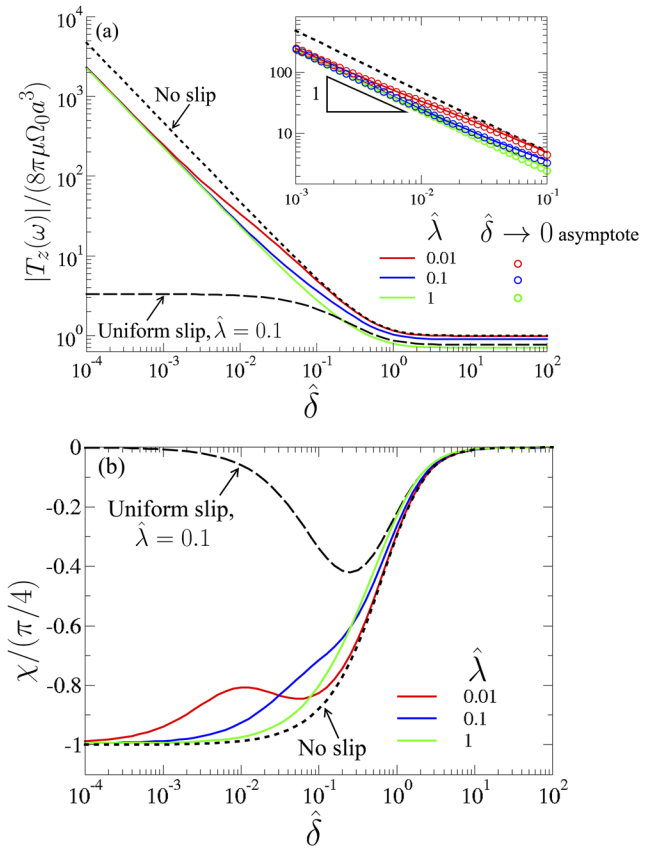


FIG. 2. (a) Plot of torque amplitude against $\hat{\delta}$ for a half cap SSJP ($\theta_0 = 90^\circ$). Calculated curves for different values of $\hat{\lambda}$ approach the same reduced Basset torque of $1/\hat{\delta}$ decay as $\hat{\delta} \rightarrow 0$, in excellent agreement with asymptotic results (symbols) evaluated from (16), as shown in the inset. (b) The phase χ basically varies from the no-slip result $\chi = -\pi/4$ to the uniform slip result $\chi = 0$ as increasing $\hat{\delta}$ from small to large values.

IV. MATCHED ASYMPTOTIC BOUNDARY LAYER THEORY

To explain the observed re-entry Basset torque and RHTT, we further develop a matched asymptotic theory to resolve how the flow behaves within a thin boundary layer when $\omega a^2/\nu$ is large. Let $\varepsilon \equiv \hat{\delta}/\sqrt{2} = (\omega a^2/\nu)^{-1/2}$ be the small parameter. We stretch the radial coordinate with $r = 1 + \varepsilon y$ and expand the azimuthal velocity as

$$w = w_0 + \varepsilon w_1 + O(\varepsilon^2). \quad (11)$$

Substituting (11) into (2) and (3), we obtain the leading order governing equation and boundary condition as

$$-i w_0 = \frac{\partial^2 w_0}{\partial y^2}, \quad (12)$$

$$w_0 - \sin \theta = \left(\frac{\beta(\theta)}{\varepsilon} \right) \frac{\partial w_0}{\partial y} \text{ at } y = 0. \quad (13)$$

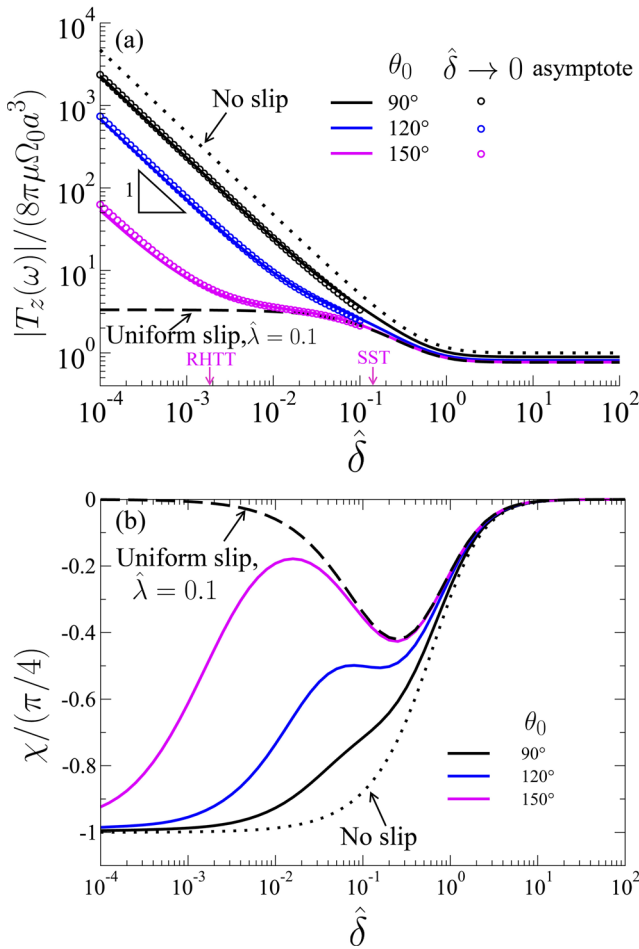


FIG. 3. (a) Plot of torque amplitude against $\hat{\delta}$ for different stick-slip partitions with $\hat{\lambda} = 0.1$. For an SSJP with a small stick portion such as $\theta_0 = 150^\circ$, in particular, mixed stick-slip effects are manifested by the coexistence of a Basset-like $1/\hat{\delta}$ decay and a slip-induced plateau, showing two transition points, RHTT and SST points, evaluated using (20) and (19), respectively. (b) The phase behaviors corresponding to (a). Compared to the other cases, the phase behavior of the $\theta_0 = 150^\circ$ case appears even more nonmonotonic.

In (13), because the effective slip coefficient β/ϵ can either vanish for the stick face or be large for the slip face, it is necessary to retain the driving slip velocity $\sin \theta$ on the left hand side so that a transition from slip to no slip can be captured when ϵ is varied.

The solution to (12) satisfying (13) is

$$w_0 = \sin \theta g(\theta) e^{-ky}, \tag{14}$$

where $k = e^{-i\pi/4}$ and $g(\theta) = (1 + k\beta(\theta)/\epsilon)^{-1}$. The shear stress is thus

$$\tau_{r\phi}(y=0) = (-k/\epsilon) \sin \theta g(\theta). \tag{15}$$

Using (8) and (15), the leading order torque amplitude can be readily determined as

$$\frac{T_z(\omega)}{-8\pi\mu\Omega_0 a^3} = \frac{1}{3\epsilon} e^{-i\pi/4} \left[g_0 - \frac{1}{5} g_2 \right] + O(\epsilon^0), \tag{16}$$

where $g_0 = (1/2) \int_{-1}^1 g(\eta) \mathcal{P}_0(\eta) d\eta$ and $g_2 = (5/2) \int_{-1}^1 g(\eta) \mathcal{P}_2(\eta) d\eta$ are the monopole and quadrupole contributions, respectively, and the functions \mathcal{P}_n represent the Legendre functions. Writing $\beta(\eta) = \hat{\lambda} \mathcal{H}(\eta - \eta_0)$ in terms of the Heaviside step function \mathcal{H} , (16) can be evaluated as

$$\frac{T_z(\omega)}{-8\pi\mu\Omega_0 a^3} = \frac{1}{3\epsilon} \frac{e^{-i\pi/4}}{(1 + k\hat{\lambda}/\epsilon)} \left[1 + \frac{k\hat{\lambda}}{\epsilon} (\eta_0 + 1)^2 C \right] + O(\epsilon^0), \tag{17}$$

where $C = (2 - \eta_0)/4$. In the $\epsilon \rightarrow 0$ limit, (17) is reduced to

$$\frac{T_z(\omega)}{-8\pi\mu\Omega_0 a^3} = \frac{1}{3\epsilon} (\eta_0 + 1)^2 C e^{-i\pi/4}. \tag{18}$$

This is exactly the reduced Basset torque shown in Figs. 2 and 3. The amplitude of this torque is found to depend only on the stick-slip partition. More importantly, the torque appears more sensitive to the coverage of the stick face, $\eta_0 + 1$. In the purely no-slip case, i.e., $\eta_0 = 1$, (18) is reduced to the usual Basset torque value $e^{-i\pi/4}/3\epsilon$.

However, if the particle is completely slipper, i.e., $\eta_0 = -1$, then (17) yields a constant torque plateau $1/3\hat{\lambda}$ for $|k\hat{\lambda}/\epsilon| \gg 1$ or for ϵ below the SST point,

$$\epsilon_{SST} \approx \hat{\lambda}. \tag{19}$$

Hence, if this slip particle is covered with a tiny stick patch (i.e., η_0 is close to -1), the slip torque plateau $1/3\hat{\lambda}$ will start to rise toward the reduced Basset torque (18) when ϵ is decreased to the RHTT point,

$$\epsilon_{RHTT} \approx \hat{\lambda} (\eta_0 + 1)^2 C. \tag{20}$$

Similar to (18), ϵ_{RHTT} is also sensitive to the coverage of the stick face. When the stick face is small, ϵ_{RHTT} will be much smaller than ϵ_{SST} . This will in turn make the torque exhibit a reduced Basset torque followed by a slip torque plateau, which explains the $\theta_0 = 150^\circ$ curve shown in Fig. 3(a). However, if the stick face is not small, ϵ_{RHTT} becomes comparable to ϵ_{SST} . The torque in the small ϵ regime will be dominated by the reduced Basset torque (18) without seeing a slip plateau, which explains Fig. 2(a).

For an arbitrary time-dependent spinning motion, we can express the angular velocity $\Omega(t)$ as a Fourier integral followed by its conversion to Laplace transform with $-i\omega \rightarrow s$. Further with the aid of the convolution theorem, we transform (17) into

$$\frac{T_z(t)}{-8\pi\mu a^3} = \frac{1}{3} \int_{-\infty}^t \frac{d\Omega(\tau')}{d\tau'} M(t - \tau') d\tau', \tag{21}$$

with the memory kernel

$$M(t) = \frac{1}{\hat{\lambda}} \exp\left(\frac{t}{\hat{\lambda}^2 t_v}\right) \operatorname{erfc}\left(\sqrt{\frac{t}{\hat{\lambda}^2 t_v}}\right) (1 - C(1 + \eta_0)^2) + \frac{C(1 + \eta_0)^2}{\sqrt{\pi}} \frac{1}{\sqrt{t/t_v}} + \dots \tag{22}$$

Here, $t_v = a^2/\nu$ is the viscous diffusion time. $\hat{\lambda}^2 t_v = \lambda^2/\nu \equiv t_{SST}$ is the SST time corresponding to (19) when the boundary layer thickness $\delta \sim (\nu t)^{1/2}$ grows to the size of the slip length λ . t_{SST} is typically shorter than t_v since $\lambda < a$.

If the particle is subjected to an impulsive rotation with $\Omega(t) = \Omega_0$ (constant), for short time $t/t_v \ll 1$, (21) is reduced to

$$\frac{T_z(t)}{-8\pi\mu\Omega_0 a^3} = \frac{C}{3\sqrt{\pi}}(\eta_0 + 1)^2 \left(\frac{t}{t_v}\right)^{-1/2} + \frac{1}{3\lambda}(1 - C(\eta_0 + 1)^2) \times \left(1 - \frac{2}{\sqrt{\pi}\lambda} \left(\frac{t}{t_v}\right)^{1/2}\right) + O(t/t_v). \quad (23)$$

As $t \rightarrow 0$, the torque will be dominated by the $(t/t_v)^{-1/2}$ term, which is exactly the reduced Basset contribution corresponding to (18). However, if the stick face is small (i.e., η_0 is close to -1), the slip torque plateau $1/3\lambda$ can become comparable to the $(t/t_v)^{-1/2}$ term. This occurs at around the RHTT time $t_{RHTT} \approx (9/16\pi)(\eta_0 + 1)^4 t_{SST}$ corresponding to (20).

V. CONCLUDING REMARKS

We have demonstrated that the viscous torque responses of an oscillatory spinning SSJP are in fact of neither no-slip nor slip type but mixed with both. Because part of the particle surface is no-slip, the response in the high frequency regime is always dominated by the reduced Basset torque that varies inversely with the Stokes boundary layer thickness δ . However, if the stick face becomes sufficiently small, the reduced Basset torque can turn into a plateau due to strong slip effects at larger values of δ prior to changing the usual no-slip Basset torque that prevails at δ greater than the slip-stick transition point $\delta \sim \lambda$. This reduced Basset to slip plateau transition and the slip-stick transition seems to be generic features for SSJPs. These features may provide more robust means for better characterizing or manipulating these heterogeneous particles.

In experimental perspectives, to our best knowledge the oscillatory spinning of an SSJP has not yet been performed experimentally. Nevertheless, we can at least provide estimates of relevant physical quantities for future realization of such an experiment. Consider an SSJP of radius $a = 100 \mu\text{m}$ undergoing rotational oscillations at the peak angular velocity Ω_0 and frequency ω in water (of density $\rho = 1 \text{ g/cm}^3$ and viscosity $\mu = 10^{-2} \text{ P}$). To ensure the rotational Reynolds number $Re = \rho\Omega_0 a^2/\mu$ to be much smaller than unity, Ω_0 has to be no greater than 10^2 s^{-1} in magnitude. Suppose $\Omega_0 \approx 10 \text{ s}^{-1}$. Hence, the steady torque is around the Stokes value $T_{Stokes} = 8\pi\mu\Omega_0 a^3 \approx 0.25 \text{ pN m}$. The viscous damping frequency $\omega_{viscous} = (2\pi)^{-1}\nu/a^2 \approx 16 \text{ Hz}$ with $\nu = \mu/\rho = 10^{-2} \text{ cm}^2/\text{s}$. The slip-stick transition will occur at $\omega_{SST} = (2\pi)^{-1}\nu/\lambda^2 = \omega_{viscous}(a/\lambda)^2$ from (19). If the slip length $\lambda \sim 1 \mu\text{m}$ which is 1% of a , $\omega_{SST} \approx 1.6 \times 10^5 \text{ Hz}$. If the SSJP has a small stick cap with $\theta_0 = 150^\circ$, a constant torque $T_{slip} = T_{Stokes}(a/3\lambda) \approx 8.33 \text{ pN m}$ will appear at frequencies higher than ω_{SST} . When ω is further increased to the re-entrant history torque transition point $\omega_{RHTT} = 4(2 - \cos\theta_0)^{-1}(\cos\theta_0 + 1)^{-2}\omega_{SST} \approx 1.2 \times 10^7 \text{ Hz}$ from (20), a reduced Basset torque will start to show up. This torque has

amplitude $T_{Basset} = T_{slip}(\omega/\omega_{RHTT})^{1/2}$ greater than T_{slip} from (18) and continues at frequencies higher than ω_{RHTT} .

ACKNOWLEDGMENTS

This work was supported by the Ministry of Science and Technology of Taiwan under Grant No. MOST 108-2811-E-006-511 of H.-H.W.

REFERENCES

- 1 A. Walther and A. H. E. Müller, "Janus particles: Synthesis, self-assembly, physical properties, and applications," *Chem. Rev.* **113**, 5194–5261 (2013).
- 2 D. G. Crowdy, "Exact solutions for cylindrical 'slip-stick' Janus swimmers in Stokes flow," *J. Fluid Mech.* **719**, R2 (2013).
- 3 A. M. Boymelgreen and T. Miloh, "A theoretical study of induced-charge dipolophoresis of ideally polarizable asymmetrically slipping Janus particles," *Phys. Fluids* **23**, 072007 (2011).
- 4 Q. Sun, E. Klaseboer, B. C. Khoo, and D. Y. Chan, "Stokesian dynamics of pill-shaped Janus particles with stick and slip boundary conditions," *Phys. Rev. E* **87**, 043009 (2013).
- 5 J. W. Swan and A. S. Khair, "On the hydrodynamics of 'slip-stick' spheres," *J. Fluid Mech.* **606**, 115–132 (2008).
- 6 A. Ramachandran and A. S. Khair, "The dynamics and rheology of a dilute suspension of hydrodynamically Janus spheres in a linear flow," *J. Fluid Mech.* **633**, 233–269 (2009).
- 7 M. Trofa, G. D'Avino, and P. L. Maffettone, "Numerical simulations of a stick-slip spherical particle in Poiseuille flow," *Phys. Fluids* **31**, 083603 (2019).
- 8 E. Yariv and M. Siegel, "Rotation of a superhydrophobic cylinder in a viscous liquid," *J. Fluid Mech.* **880**, R4 (2019).
- 9 Z. Ye, E. Diller, and M. Sitti, "Micro-manipulation using rotational fluid flows induced by remote magnetic micro-manipulators," *J. Appl. Phys.* **112**, 064912 (2012).
- 10 C. P. Moerland, L. J. van IJzendoorn, and M. W. J. Prins, "Rotating magnetic particles for lab-on-chip applications—A comprehensive review," *Lab Chip* **19**, 919–933 (2019).
- 11 A. B. Basset, "On the motion of a sphere in a viscous liquid," *Philos. Trans. R. Soc., A* **179**, 43–63 (1888).
- 12 L. D. Landau and E. M. Lifshitz, *Fluid Mechanics*, 2nd ed. (Pergamon, New York, 1987).
- 13 H. Fujioka and H.-H. Wei, "Letter: New boundary layer structures due to strong wall slippage," *Phys. Fluids* **30**, 121702 (2018).
- 14 A. R. Premlata and H.-H. Wei, "The Basset problem with dynamic slip: Slip-induced memory effect and slip-stick transition," *J. Fluid Mech.* **866**, 431–449 (2019).
- 15 E. A. Ashmawy, "Unsteady rotational motion of a slip spherical particle in a viscous fluid," *ISRN Math. Phys.* **2012**, 1–8.
- 16 A. Premlata and H.-H. Wei, "Re-entrant history force transition for stick-slip Janus swimmers: Mixed Basset and slip-induced memory effects," *J. Fluid Mech.* **882**, A7 (2020).
- 17 K. B. Ranger, "Slow viscous flow past a rotating sphere," *Math. Proc. Cambridge Philos. Soc.* **69**, 333–336 (1971).
- 18 N. Riley, "Steady streaming," *Annu. Rev. Fluid Mech.* **33**, 43–65 (2001).